Summer School on Mathematical Control Theory

(3 - 28 September 2001)

Optimizing bioreactors by extremum seeking

Georges Bastin

CESAME
Center for Systems Engineering and Applied Mechanics
Bâtiment Euler
4, Avenue G. Lemaitre
B-1348 Louvain
Belgium

OPTIMIZING BIOREACTORS BY EXTREMUM SEEKING

HSIN-HSIUNG WANG[1,†], MIROSLAV KRSTIĆ[2,*] AND GEORGES BASTIN[3]

[1]*Department of Electrical Engineering, Oriental Institute of Technology, 58, sec. 2, Szu-Chuan Road, Panchiao,
Taipei County 220, Taiwan*
[2]*Department of AMES, UC San Diego, La Jolla, CA 92093-0411, U.S.A.*
[3]*CESAME-Center for Systems Engineering and Applied Mechanics, Université Catholique de Louvain,
Louvain-la-Neuve, Belgium*

SUMMARY

The optimization of the operation of biological reactors is an interesting non-linear problem whose solution offers potential economic benefit. We apply a peak seeking method to approach the maximum biomass production rate in a continuous stirred tank bioreactor. Two models, Monod and Haldane, are investigated and it is shown by simulation that the peak seeking scheme achieves optimization for both cases. A stabilizing feedback controller with a washout filter is designed to extend the operating range for the Haldane model. Copyright © 1999 John Wiley & Sons, Ltd.

1. INTRODUCTION

The application of modern model-based techniques for optimization and control of bioreactors is hampered by a major bottleneck: the difficulty of identifying reliable first principle models for these highly non-linear and widely uncertain systems.

It is, however, recognized that even small performance improvements may result in substantial economic benefits. It is the purpose of this paper to present an 'extremum seeking' approach for the optimization of bioreactors which allows for an automated seeking of the best operating point while being robust against a complete uncertainty regarding the process kinetics.

An extensive introduction into the modelling and control issues for bioreactors can be found in the tutorial paper.[1] For the feedback control of these processes, in order to cope with the modelling uncertainties, adaptive techniques have been mainly investigated in the literature (see e.g. Reference 2–4) including more recently adaptive neural network model.[5-7]

This paper was submitted for publication by editor E. Mosca

*Correspondence to: Professor Miroslav Krstić, Department of AMES, UC San Diego, La Jolla, CA 92093-0411, U.S.A.,
E-mail: mkrstic@ames.ucsd.edu

†This work was performed while the first author was a PhD student with M. Krstić at the University of Maryland.

In the present paper, in order to maximize the productivity of a continuous stirred tank bioreactor, we apply *extremum seeking* which is an old adaptive non-linear control method from the 50–60s whose stability proof we provided just recently in Reference 8 (and tested it experimentally on an axial-flow compressor[9]). Compared to classical adaptive and neural net methods, the main advantages of our approach are twofold: first the optimization objective (productivity maximization) is an explicit ingredient of the formulation of the adaptive control law, i.e. the optimization objective is guaranteed to be achieved when the control is convergent; second, this approach does not require any parameterization nor structural formalization of the modelling uncertainty (even under the form of a black box model like neural nets).

As a benchmark for our demonstration, we use a simple model of a continuous stirred tank biological reactor with numerical parameter values from References 10 and 11. The optimization objective is to maximize the biomass production, more precisely the mass outflow rate of produced microorganisms. The steady states of the process can be characterized by a non-monotonic map relating the biomass production to the dilution rate which is our control input. The purpose of the extremum seeking method is to iteratively adjust the dilution rate in order to steer the process to the maximum of the map which corresponds to a maximum productivity.

The paper is organized as follows. In Section 2 we describe the dynamical model of the bioreactor under consideration, with Monod and Haldane kinetics and in Section 3 we state the control objective. In Section 4, we study the open-loop stability of these models. We apply extremum seeking to the system in Section 5 and show simulation results. In Section 6 we design a stabilizing controller with a washout filter to extend the operating range for the Haldane model.

2. THE DYNAMIC MODEL OF A CONTINUOUS STIRRED TANK REACTOR

In this section, we present the dynamic model of a continuous stirred tank bioreactor where a single population of micro-organisms is cultivated on a single limiting substrate. The bioreactor is shown in Figure 1.
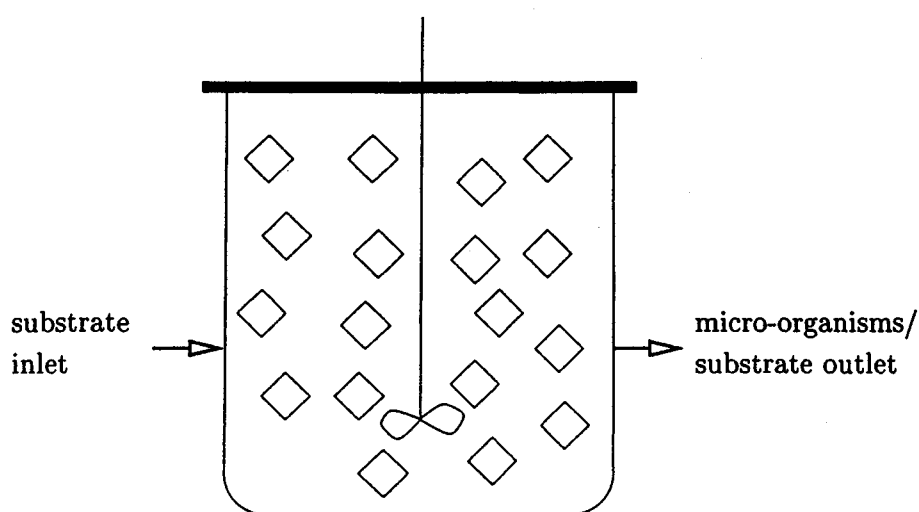

Figure 1. Bioreactor with continuous culture

The limiting substrate is fed into the culture vessel with a constant concentration s_R at a volumetric flow rate f. The culture medium is withdrawn at the same volumetric rate f so that the culture volume v in the vessel is kept constant. The dilution rate D is defined as $D = f/v$ and is the inverse of the residence time.

It is assumed that the other required substrates (including oxygen if needed) are provided in excess, that the culture medium is perfectly mixed and that the environmental conditions (temperature and pH) are regulated at appropriate constant values.

The dynamic behaviour of this bioreactor is then described by the following standard mass balance model (see e.g. Reference 2):

$$\dot{x} = \mu(s)x - Dx \tag{1}$$

$$\dot{s} = D(s_R - s) - \frac{\mu(s)x}{Y} \tag{2}$$

where x is the biomass concentration, s is the substrate concentration, $\mu(s)$ is the specific growth rate function and Y is the yield coefficient.

Many analytical expressions for the function $\mu(s)$ have been proposed empirically or experimentally and we consider the two most commonly used, but many others could be considered as well. The most classical function is the Monod model:

$$\mu(s) = \mu_m \left(\frac{s}{K_s + s} \right) \tag{3}$$

where μ_m is the maximum growth rate constant and K_s is a saturation constant. If substrate inhibition is considered, the function $\mu(s)$ may be given by the Haldane model:

$$\mu(s) = \frac{\mu_m}{1 + K_s/s + s/K_i} \tag{4}$$

where K_i is an inhibition constant.

Hence, for Monod kinetics the bioreactor model is:

$$\dot{x} = x \left(\frac{\mu_m s}{K_s + s} - D \right) \tag{5}$$

$$\dot{s} = D(s_R - s) - \frac{\mu_m}{Y} \left(\frac{x_s}{K_s + s} \right) \tag{6}$$

and for Haldane kinetics the model is

$$\dot{x} = x \left(\frac{\mu_m}{1 + K_s/s + s/K_i} - D \right) \tag{7}$$

$$\dot{s} = D(s_R - s) - \frac{\mu_m}{Y} \frac{x}{1 + K_s/s + s/K_i} \tag{8}$$

To normalize the model, we use $Ys_R, s_R, \mu_m, 1/\mu_m$ as the units of x, s, D and t, respectively. So the non-dimensional models become

$$\dot{x} = x\left(\frac{s}{K_1 + s} - D\right) \tag{9}$$

$$\dot{s} = D(1 - s) - \frac{xs}{K_1 + s} \tag{10}$$

for Monod model and

$$\dot{x} = x\left(\frac{1}{1 + K_1/s + s/K_2} - D\right) \tag{11}$$

$$\dot{s} = D(1 - s) - \frac{x}{1 + K_1/s + s/K_2} \tag{12}$$

for Haldane model, where $K_1 = K_s/s_R$ and $K_2 = K_i/s_R$.

3. THE OPTIMIZATION OBJECTIVE

Let us assume that the industrial goal of the process is the production of micro-organisms. As an optimization objective, it is then natural to consider the maximization of the amount of biomass harvested per unit of time which can be measured by the biomass outflow rate:

$$y = xD \tag{13}$$

We shall see in the next section that the steady states of the process are characterized by a non-monotonic map relating the biomass outflow rate (the controlled output) y to the dilution rate D which is our control input. The purpose of the extremum seeking method is then to iteratively adjust the dilution rate in order to steer the process to the maximum of this map.

It is important to understand that we do *not* assume that the function $\mu(s)$ is *a priori* known: the Monod and Haldane models presented above must be viewed as a theoretical benchmark to illustrate and analyse the efficiency of the extremum seeking approach. Our aim will be to show that the best operating point can be discovered by a peak seeking algorithm which is completely 'ignorant' of the form of the kinetics.

4. BIFURCATION ANALYSIS OF THE OPEN-LOOP SYSTEM

4.1. Monod model

To investigate the stability of the open-loop system with a Monod model, we first calculate equilibria corresponding to a constant dilution rate $D = D_0$. Let the right-hand side of (9) and (10) be zero, after some calculations we obtain two equilibria; one is ($x_0 = 0, s_0 = 1$) and the other can

be expressed as a function of D_0 as follows:

$$s_0 = \frac{K_1 D_0}{1 - D_0} \tag{14}$$

$$x_0 = \frac{1 - (1 + K_1)D_0}{1 - D_0} \tag{15}$$

The equilibrium ($x_0 = 0$, $s_0 = 1$) is called the *wash-out* steady state since the concentration of the micro-organism is reduced to zero.

The Jacobian of the system at (x_0, s_0) is

$$J = \begin{bmatrix} \dfrac{s_0}{K_1 + s_0} - D_0 & \dfrac{K_1 s_0}{(K_1 + s_0)^2} \\ -\dfrac{s_0}{K_1 + s_0} & -\dfrac{K_1 x_0}{(K_1 + s_0)} - D_0 \end{bmatrix} \tag{16}$$

It is easy to show that

1. The wash-out equilibrium ($x_0 = 0$, $s_0 = 1$) is stable when $D_0 > 1/(1 + K_1)$ and unstable when $D_0 < 1/(1 + K_1)$.
2. At the other equilibrium, the Jacobian can be written as

$$J = \begin{bmatrix} 0 & B - D_0 \\ -D_0 & -B \end{bmatrix} \tag{17}$$

where

$$B \triangleq \frac{(1 - D_0)^2}{K_1} + D_0^2 \tag{18}$$

This equilibrium is defined only for $D_0 < 1/(1 + K_1)$ and is stable for all the values of D_0 for which it is defined.

The steady-state output can be expressed as

$$y_0 = \frac{D_0(1 - (1 + K_1)D_0)}{1 - D_0} \tag{19}$$

To obtain the extremum value y_0^* of y_0 we differentiate (19) with respect to D_0 and get

$$D^* = 1 - \sqrt{\frac{K_1}{1 + K_1}} \tag{20}$$

$$s^* = \sqrt{K_1(1 + K_1)} - K_1 \tag{21}$$

$$x^* = 1 + K_1 - \sqrt{K_1(1 + K_1)} \tag{22}$$

For bifurcation analysis we select the parameters provided by Herbert *et al.*[10] as: $\mu_m = 1\,\text{h}^{-1}$, $Y = 0.5$, $K_s = 0.2\,\text{g/l}$, $s_R = 10\,\text{g/l}$, $s_R = 10\,\text{g/l}$. So $K_1 = K_s/s_R = 0.02$. By substituting K_1 into (20)–(22), we get

$$y_0^* = 0.754 \quad \text{for} \quad D^* = 0.860, \quad s^* = 0.123, \quad x^* = 0.877. \tag{23}$$

Since the second derivative of y_0 with respect to D_0 is negative, this point is a maximum. The bifurcation diagram parameterized by the dilution rate for the steady-state output is shown in Figure 2 in which the solid line represents stable equilibria and the dashed line represents unstable equilibria.

4.2. Haldane model

To study the stability of the open-loop system with Haldane model, we also calculate equilibria corresponding to a constant dilution rate $D = D_0$. Let the right-hand side of (11) and (12) be zero. Calculations show that the system has a unique equilibrium or multiple equilibria, depending on the value of D_0. The wash-out state always exists, i.e. $(x_0 = 0, \quad s_0 = 1)$. For $D_0 < 1/(1 + 2\sqrt{K_1/K_2})$ there are two additional equilibria:

$$x_{01} = 1 - s_{01}$$

$$s_{01} = \frac{K_2(1 - D_0)}{2D_0} - \frac{1}{2}\sqrt{\left(\frac{K_2(1 - D_0)}{D_0}\right)^2 - 4K_1K_2} \tag{24}$$

$$x_{02} = 1 - s_{02}$$

$$s_{02} = \frac{K_2(1 - D_0)}{2D_0} + \frac{1}{2}\sqrt{\left(\frac{K_2(1 - D_0)}{D_0}\right)^2 - 4K_1K_2} \tag{25}$$
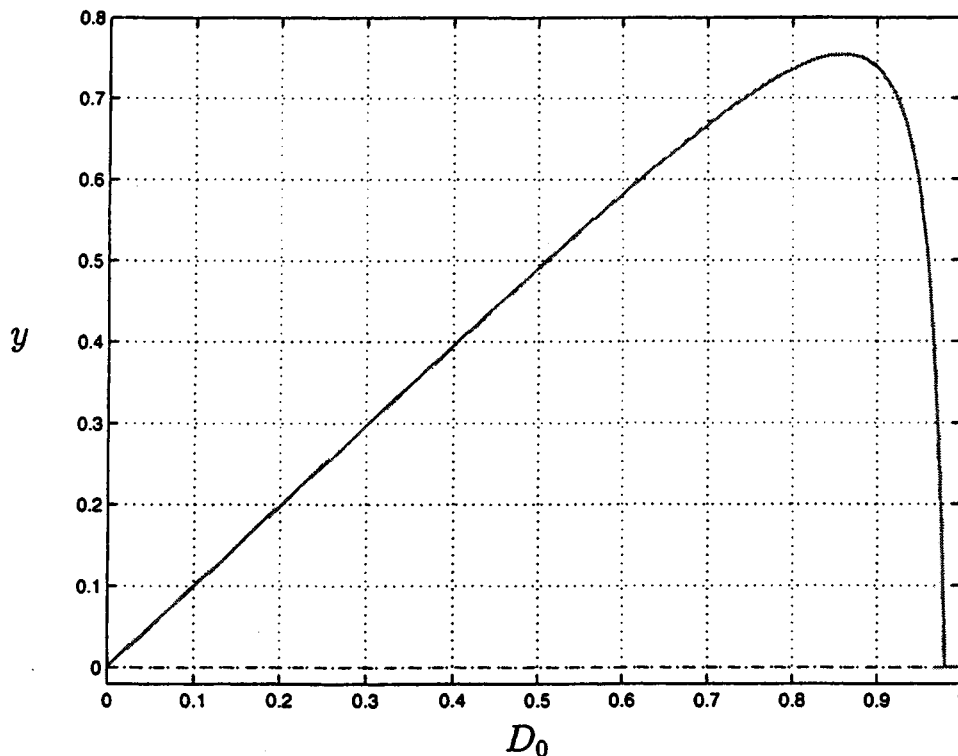
Figure 2. The bifurcation diagram of output of micro-organism w.r.t. dilution rate for a Monod model

The Jacobian at (x_0, s_0) is

$$
J = \begin{bmatrix} \dfrac{1}{1 + K_1/s_0 + s_0/K_2} - D_0 & -\dfrac{x_0(1/K_2 - K_1/s_0^2)}{(1 + K_1/s_0 + s_0/K_2)^2} \\[2ex] -\dfrac{1}{1 + K_1/s_0 + s_0/K_2} & -D_0 + \dfrac{x_0(1/K_2 - K_1)/s_0^2)}{(1 + K_1/s_0 + s_0/K_2)^2} \end{bmatrix}
\tag{26}
$$

It is easy to show that

1. The wash-out equilibrium $(x_0 = 0, s_0 = 1)$, is stable for $D_0 > (1 + 2/K_2)/(1 + K_1 + 1/K_2)^2$ and unstable for $D_0 < (1 + 2/K_2)/(1 + K_1 + 1/K_2)^2$.
2. At the other branch of equilibria, the Jacobian is

$$
J = \begin{bmatrix} 0 & -H \\ -D_0 & -D_0 + H \end{bmatrix}
\tag{27}
$$

where

$$
H \triangleq x_0 D_0^2 \left(\frac{1}{K_2} - \frac{K_1}{s_0^2} \right)
\tag{28}
$$

We choose the parameters proposed by D'Ans and Kokotović,[11] $K_1 = 0\cdot1$ and $K_2 = 0\cdot5$. Substituting these values into the Jacobian *at the maximum point*, it becomes

$$
J = \begin{bmatrix} 0 & 0\cdot5099 \\ -0\cdot5099 & -1\cdot01977 \end{bmatrix}
\tag{29}
$$

It is easy to check that the Jacobian is Hurwitz. A complete stability analysis along equilibria is shown in Figure 3.

The steady-state output can be expressed as

$$
y_0 = D_0 \left(1 - \frac{K_2(1 - D_0)}{2D_0} \pm \frac{1}{2} \sqrt{\left(\frac{K_2(1 - D_0)}{D_0} \right)^2 - 4K_1 K_2} \right)
\tag{30}
$$

To obtain the extremum value of y_0 we differentiate (30) with respect to D_0 and get

$$
D^* = \frac{K_2 s^*}{(s^*)^2 + K_2 s^* + K_1 K_2}
\tag{31}
$$

$$
s^* = \frac{\sqrt{K_1^2 K_2^2 + K_1 K_2^2 + K_1 K_2} - K_1 K_2}{1 + K_2}
\tag{32}
$$

$$
x^* = 1 - \frac{\sqrt{K_1^2 K_2^2 + K_1 K_2^2 + K_1 K_2} - K_1 K_2}{1 + K_2}
\tag{33}
$$

Substituting the values of K_1 and K_2 into (31)–(33), the maximum output is

$$
y^* = 0\cdot4322 \quad \text{for} \quad D^* = 0\cdot5099, \quad s^* = 0\cdot1523, \quad x^* = 0\cdot8477.
\tag{34}
$$

Since the second derivative is negative this point is a maximum. The bifurcation diagram for the output equilibrium parameterized by the dilution rate is shown in Figure 3.
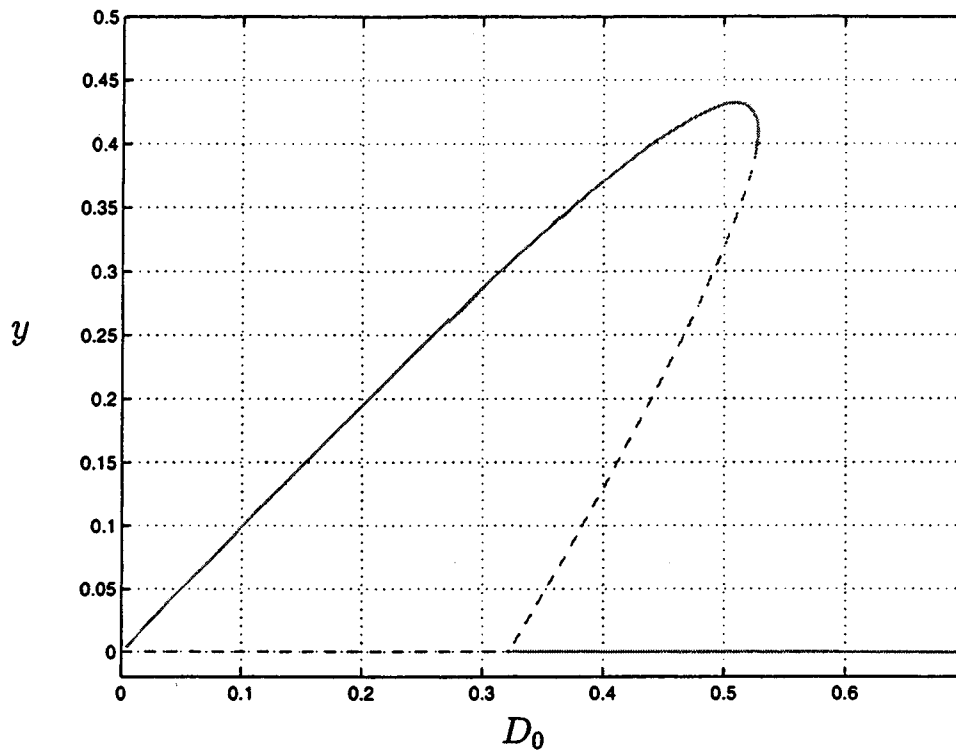
Figure 3. The bifurcation diagram of output of micro-organism w.r.t. dilution rate for a Haldane model

5. PEAK SEEKING VIA THE DILUTION RATE

Owing to the uncertainty and time-varying properties of biological processes the maximum operating point is hard to predict precisely. It is therefore of interest to implement peak seeking control which is model-free and able to automatically tune the dilution rate in the right direction. A block diagram for peak seeking implemented on a bioreactor is shown in Figure 4. The output performance index is the biomass outflow rate. The parameters are chosen as follows:

$$\text{speed of non-linear dynamics} = O(1) \gg \omega \gg \omega_h, a, k \tag{35}$$

The scheme from Figure 4 guarantees the following stability result *outlined* in the following theorem. For a detailed statement of the result and a proof the reader is urged to consult Reference 8.

Theorem 5.1.

Consider the feedback system in Figure 4 and assume that the bioreactor dynamic model has the following properties:

(1) for D in an interval $[D_1, D_2]$ there is an isolated one-dimensional manifold[†] of equilibria E(D) which depends smoothly on D;

(2) each of the equilibria in $E([D_1, D_2])$ are exponentially stable[‡] with an $O(1)$ rate of decay;
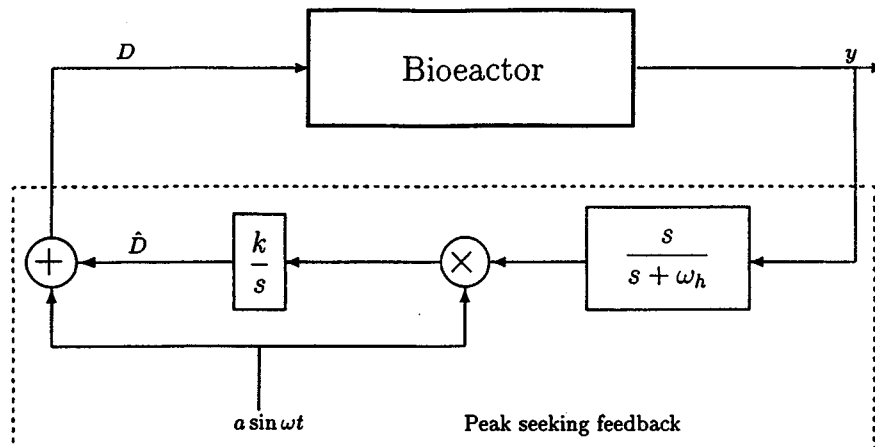
[†]Possibly more than one.
[‡]Possibly only locally.

Figure 4. Peak seeking scheme for the bioreactor.

(3) the equilibrium value of the output y on $E(\{D_1, D_2\})$ is a smooth function of D with a maximum at $D = D^*$.

Then there exists a ball of initial conditions§ around the equilibrium corresponding to $D = D^*$ and a positive constant $\bar{\omega} \ll 1$ such that, for all $\omega \in (0, \bar{\omega})$ and all a, k, $\omega_h \ll \omega$, the solution converges to an $O(\omega)$ neighbourhood of that equilibrium.

The conditions of this theorem are all verified by the analysis and bifurcation plots in the last section. It should be noted however that, in the case of the Haldane model (Figure 3), the stable interval near the peak is narrow so an additional inner feedback loop is needed to broaden it.

We now demonstrate by simulations the ability of peak seeking to adapt the dilution rate to optimize the biomass flow rate. We apply the (same) scheme to both the Monod and the Haldane model.

5.1. Monod model

For the Monod model, from Figure 2 we know that the peak occurs at $D^* = 0.86$, $s^* = 0.123$, $x^* = 0.877$. Our purpose is to tune D to D^*. We implement the peak seeking scheme with the following choice of parameters:

$$\omega_h = 0.04, \quad \omega = 0.08, \quad a = 0.03, \quad k = 5$$

First, we start from an initial dilution rate lower than the optimum rate. Figure 5 shows how the peak seeking approaches the peak along the equilibrium curve. The time response of the output is shown in Figure 6 and the time response of the tuning parameter is shown in Figure 7. The second simulation starts from a dilution rate larger than the optimum value. The results are shown in Figures 8-10.

From Figure 6, the settling time is 272 h and the improvement in performance to the maximum output is 26.7%, which means the performance is improved with a rate of about 0.1% h^{-1}. This rate of improvement is satisfactory but it is certainly not impressive. Since the time constants of

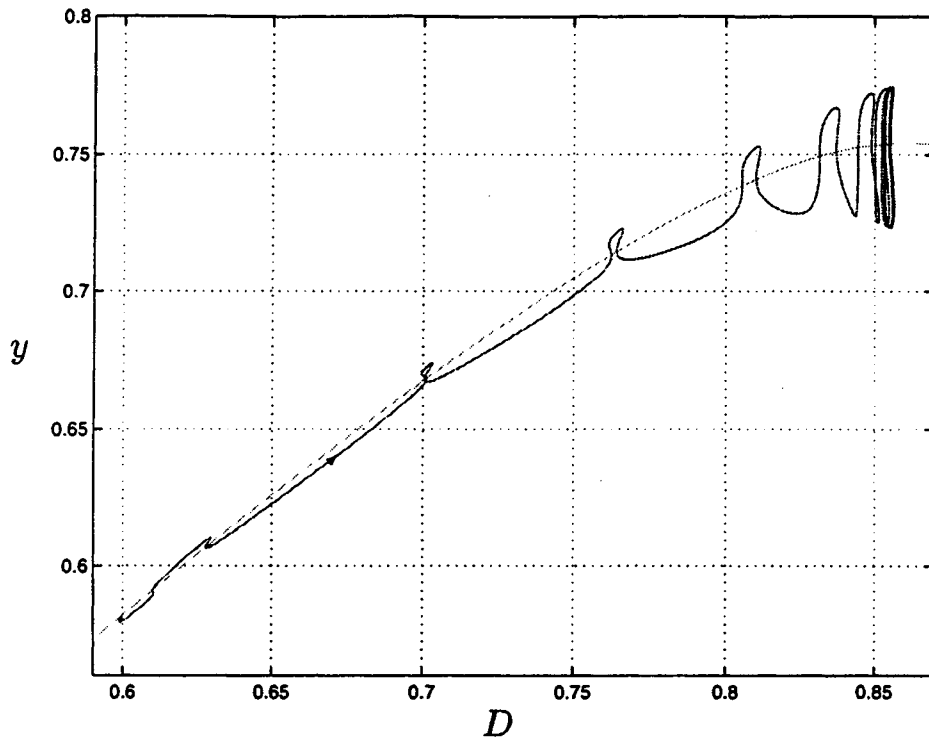§In the state space of the overall feedback system in Figure 4.

Figure 5. The maximum seeking process for the Monod model with initial dilution rate $D_0 = 0.6$
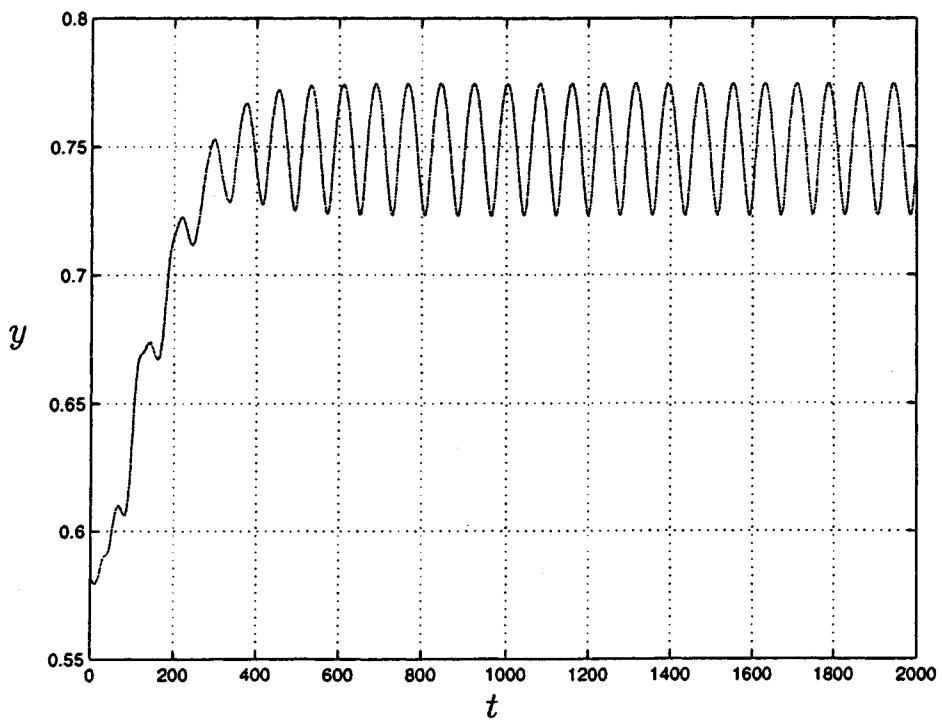

Figure 6. The time response of the output with peak seeking for the Monod model with initial dilution rate $D_0 = 0.6$
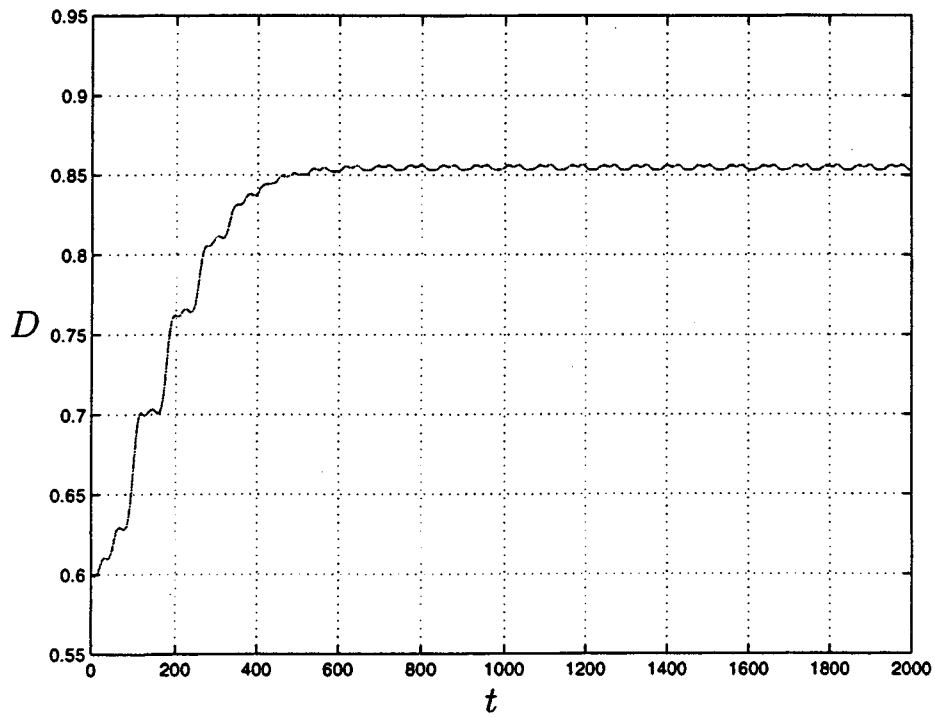
Figure 7. The time response of the tuning parameter with peak seeking for the Monod model with initial dilution rate $D_0 = 0.6$
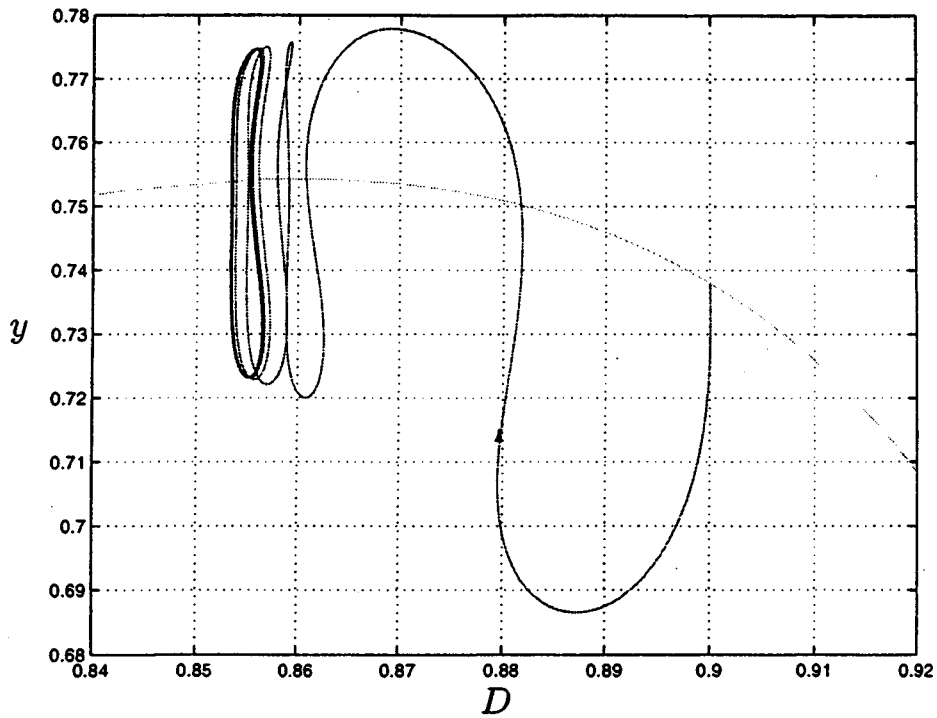

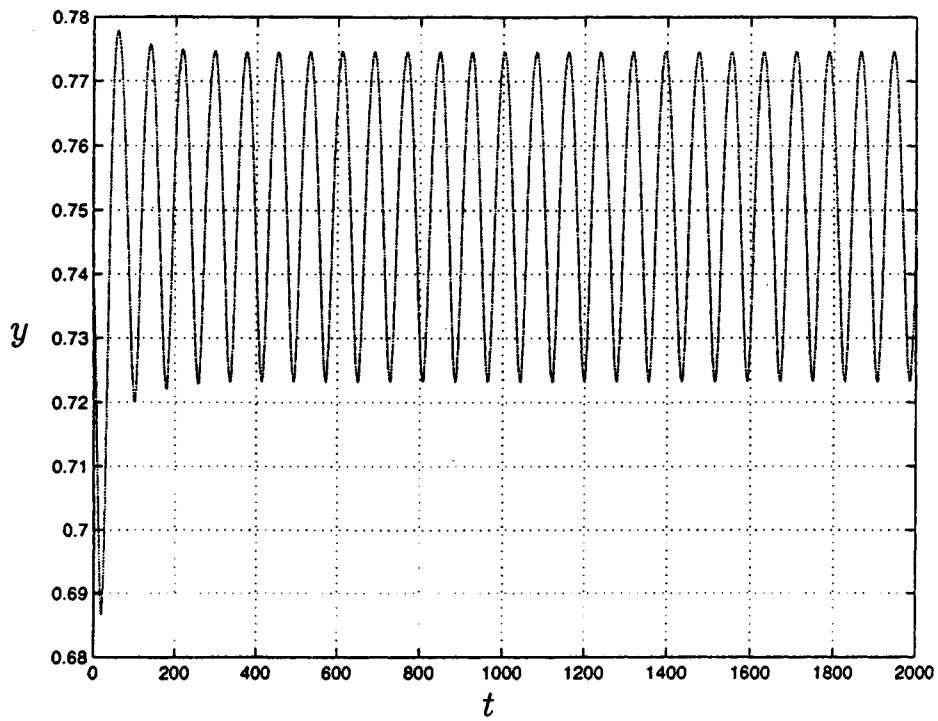Figure 8. The maximum seeking process for the Monod model with initial dilution rate $D_0 = 0.9$

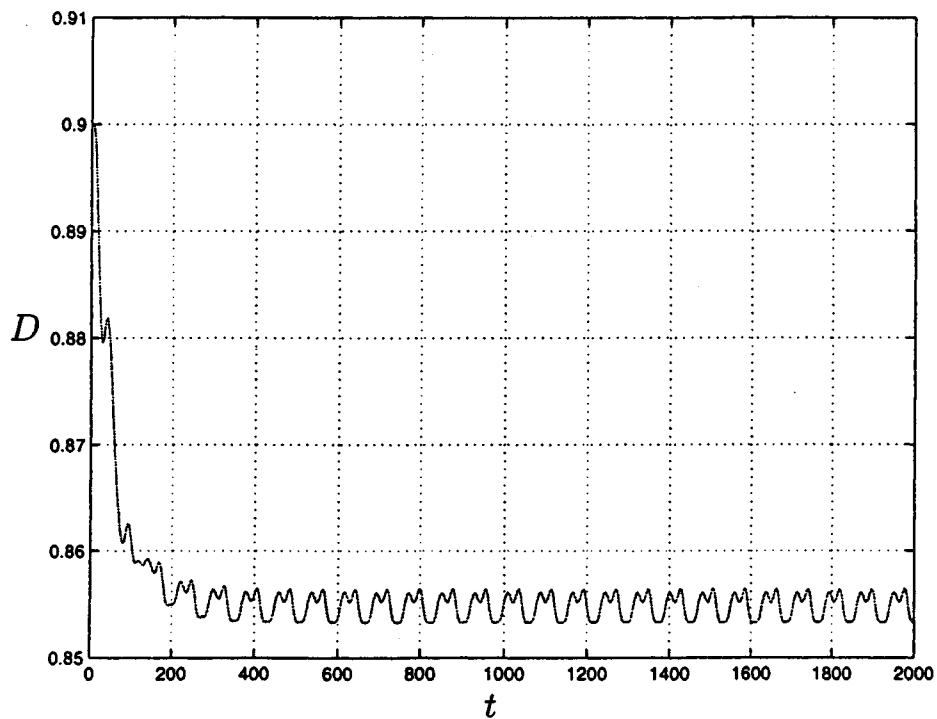Figure 9. The time response of the output with peak seeking for the Monod model with initial dilution rate $D_0 = 0{\cdot}9$

Figure 10. The time response of the tuning parameter with peak seeking for the Monod model with initial dilution rate $D_0 = 0{\cdot}9$

the system at the peak are on the order of 10, this means that the convergence to the peak takes about 27 time constants. The convergence to the peak can be made faster by tuning the parameters of the scheme and by introducing an appropriate phase shift in the perturbation sinusoid. However, we do not do this here for two reasons. First, our primary objective is to qualitatively demonstrate the possibility of finding the peak, and not to optimize the transients. Second, and more important, if we chose parameters which make the convergence from the left side of the peak faster, they are too agressive for the right side of the peak and may lead to instability. As evident by comparing Figures 6 and 9, the same parameters which result in relatively slow convergence from the left, result in fast convergence from the right. Since we do not assume to know the location of the peak, the adaptation must proceed cautiously.

The oscillations of the output y in Figure 6 are about 3% of the peak equilibrium value of y.

5.2. Haldane model

For the Haldane model, from Figure 3 we know that the peak occurs at $D^* = 0.5099$, $s^* = 0.1523$, $x^* = 0.8477$, $y^* = 0.4322$. Again our purpose is to tune D to D^*. We implement the peak seeking scheme with the same parameters as in the case of the Monod model.

First, we start from an initial dilution rate lower than the optimum value. Figure 11 shows how the peak seeking approaches the peak along the equilibrium curve. The time response of the output is shown in Figure 12 and the time response of the tuning parameter is shown in Figure 13. If we increase the initial D_0 to the right of the optimum value, the time response of the output in Figure 14 shows that *the system falls to the wash-out steady state*. This is because the Haldane model has unstable equilibria underneath the maximum point. This motivates us to apply
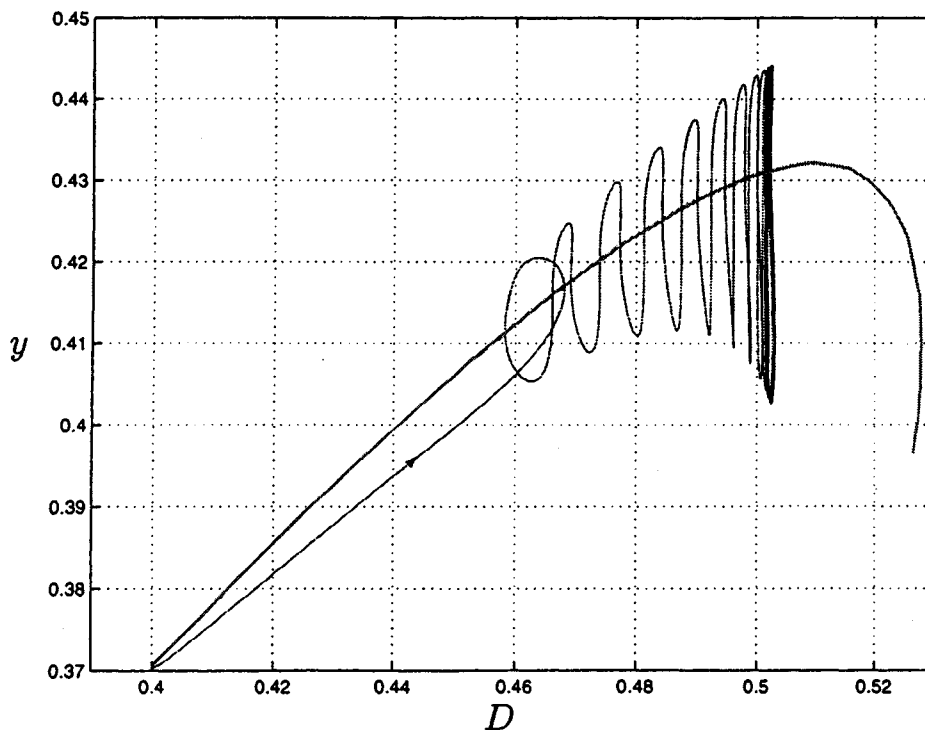

Figure 11. The maximum seeking process for the Haldane model with initial dilution rate $D_0 = 0.4$
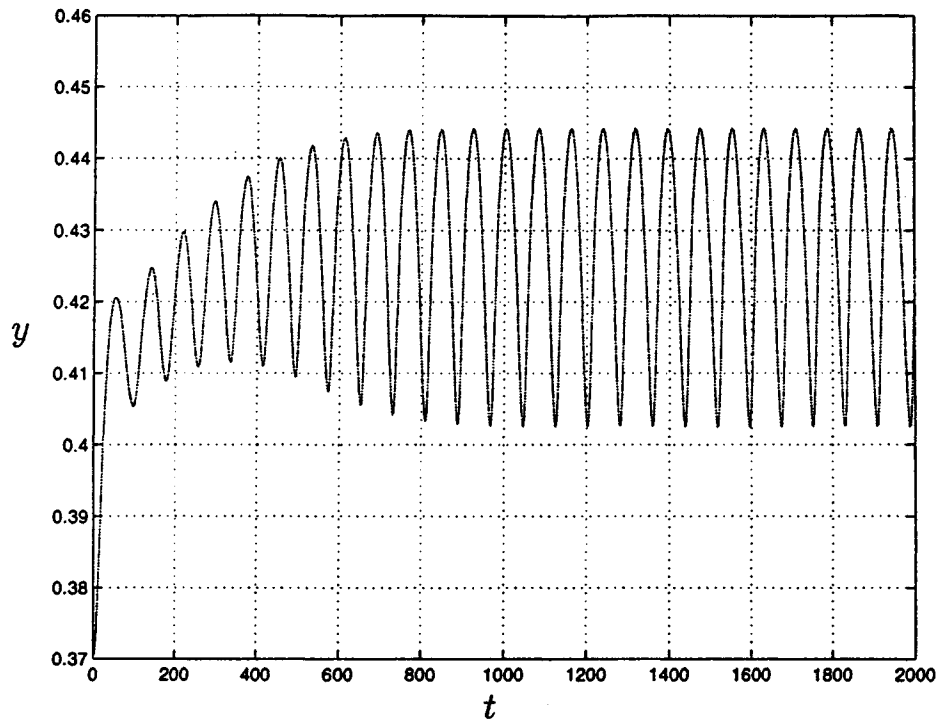
Figure 12. The time response of the output with peak seeking for the Haldane model with initial dilution rate $D_0 = 0.4$
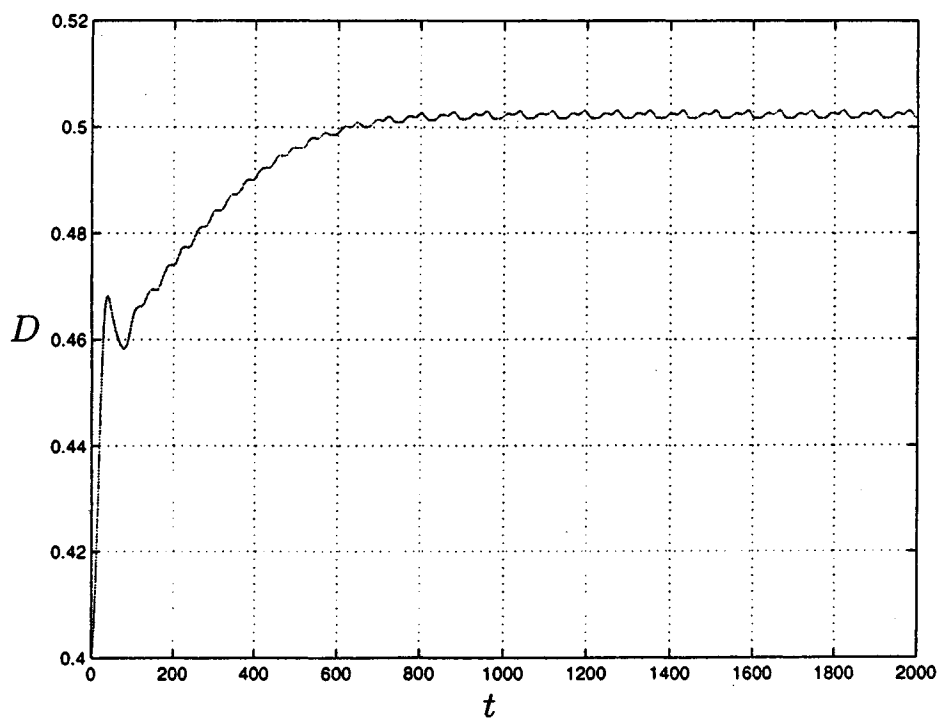
Figure 13. The time response of the tuning parameter with peak seeking for the Haldane model with initial dilution rate $D_0 = 0.4$
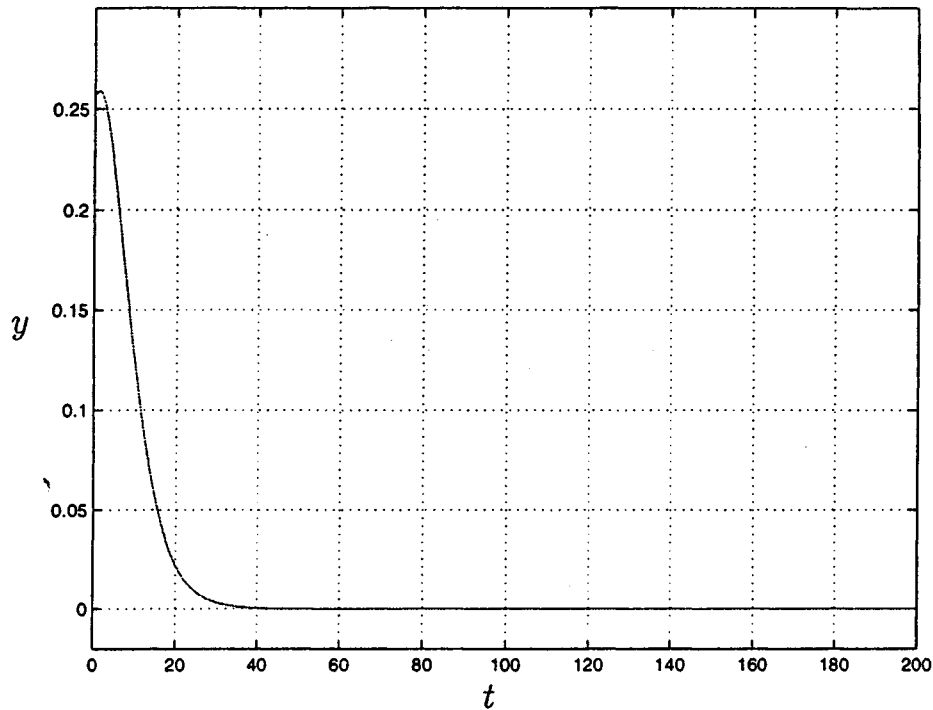

Figure 14. The time response of the output with peak seeking for the Haldane model with initial dilution rate $D_0 = 0.52$. The system starts at an unstable equilibrium and *falls into the wash-out steady state*

feedback control to stabilize the equilibrium branch under the maximum point, which is the subject of Section 6.

6. FEEDBACK WITH WASHOUT FILTERS FOR THE HALDANE MODEL

In general, a washout filter

$$W(s) = \frac{s}{s + \omega_s} \tag{36}$$

is a high pass filter that preserves the equilibrium structure and affects only the transient response and stability type. In this application, one would use it in stabilization of unstable equilibria (such as those in Figure 3) without changing their location. Clearly, a washout filter alone is not sufficient for stabilization — it is used in combination with a state feedback controller, where the states include both mean values and regulation errors, for the purpose of 'washing out' the mean values from the feedback signal. It is very important not to confuse the terms *wash-out equilibria* with *wash-out filter*. It is an unfortunate coincidence that both terms are independently broadly adopted and they both appear in this problem. Note also that, incidentally, the peak seeking scheme itself incorporates a wash-out filter $s/(s + \omega_h)$ which is used to eliminate the DC component of the output in peak seeking. This washout filter should not be confused with washout filters used in this section.

We therefore assume the full state is measurable, design a full state feedback $(D = k_x x + k_s s)$, and then apply it through washout filters as follows:

$$D = D_e + k_x(x - x_s) + k_s(s - s_s) \tag{37}$$

$$\dot{x}_s = \omega_s x_s + \omega_s x \tag{38}$$

$$\dot{s}_s = \omega_s s_s + \omega_s s \tag{39}$$

where D_e represents the equilibrium value of the control variable.

6.1. Control design

The Jacobian for the closed-loop system (x, s, x_s, s_s) at the equilibrium (x_0, s_0, x_0, s_0) is

$$J = \begin{bmatrix} -k_x x_0 & -\dfrac{x_0(1/K_2 - K_1/s_0^2)}{(1 + K_1/s_0 + s_0/K_2)^2} - k_s x_0 & k_x x_0 & k_s x_0 \\[3mm] k_x x_0 - D_e & -D_e + k_s x_0 + \dfrac{x_0(1/K_2 - K_1/s_0^2)}{(1 + K_1/s_0 + s_0/K_2)^2} & -k_x x_0 & -k_s x_0 \\[3mm] \omega_s & 0 & -\omega_s & 0 \\[3mm] 0 & \omega_s & 0 & -\omega_s \end{bmatrix} \tag{40}$$

The eigenvalues of this fourth-order matrix are hard to calculate. However, we know that the eigenvalues are continuous. Therefore, for small ω_s, two of the eigenvalues will be approximately ω_s, and the other two will be approximately equal to the eigenvalues of the closed-loop system without washout filters. The characteristic polynomial at the peak is readily shown to be (using the values in Reference 11)

$$p(\lambda) = \lambda^2 + (0\cdot8477(k_x - k_s) + 1\cdot0198)\lambda + 0\cdot4322(k_x - k_s) + 0\cdot26 \tag{41}$$

By Routh–Hurwitz method, the stability condition is

$$k_x - k_s + 1\cdot20 > 0 \quad \text{and} \quad k_x + k_s < 0\cdot60 \tag{42}$$

By choosing $k_x = 0$ and $k_s = -0\cdot2$, stability condition (42) is satisfied. The bifurcation diagram with D_e as the parameter is shown in Figure 15. Note that a small amount of gain is sufficient to stabilize the whole branch of equilibria under the maximum point. We will use this feedback gain for the peak seeking simulation.

6.2. Simulation results

As the starting point selected from Section 5.2, the initial dilution rate is 0·52. The parameters are selected as follows:

$$k_x = 0, \quad k_s = -0\cdot2, \quad \omega_h = 0\cdot04, \quad \omega = 0\cdot08, \quad a = 0\cdot03, \quad k = 2, \quad \omega_s = 0\cdot01$$

The seeking process is shown in Figure 16 and the time responses for the output y and the tuning parameter D are shown in Figures 17 and 18, respectively. The peak seeking, combined with
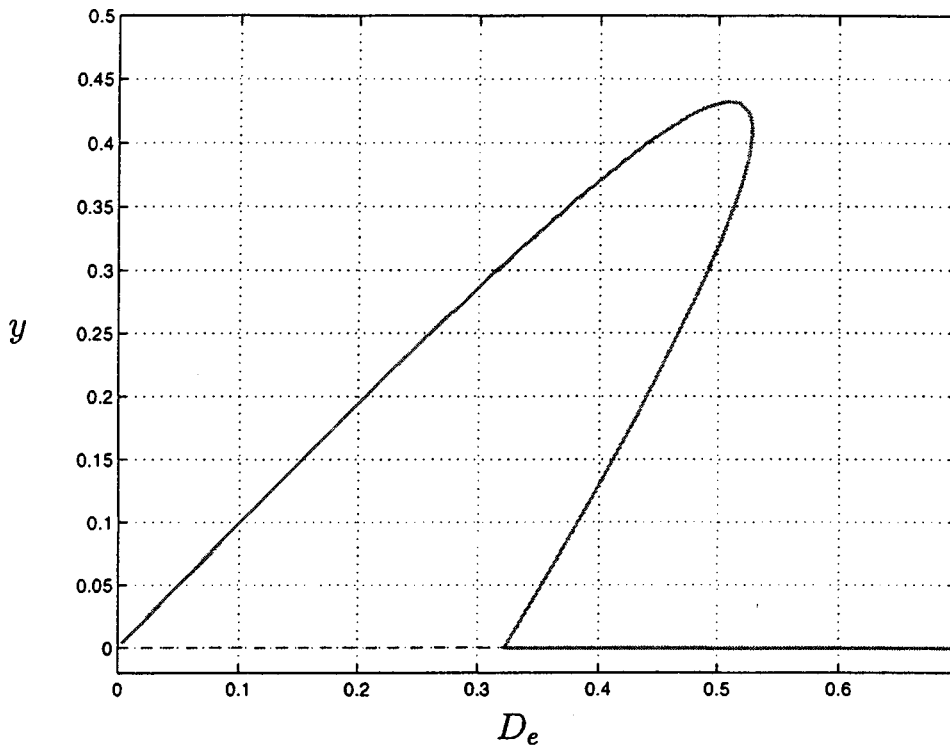
Figure 15. The bifurcation diagram of output of micro-organism w.r.t. dilution rate for a Haldane model with washout filters
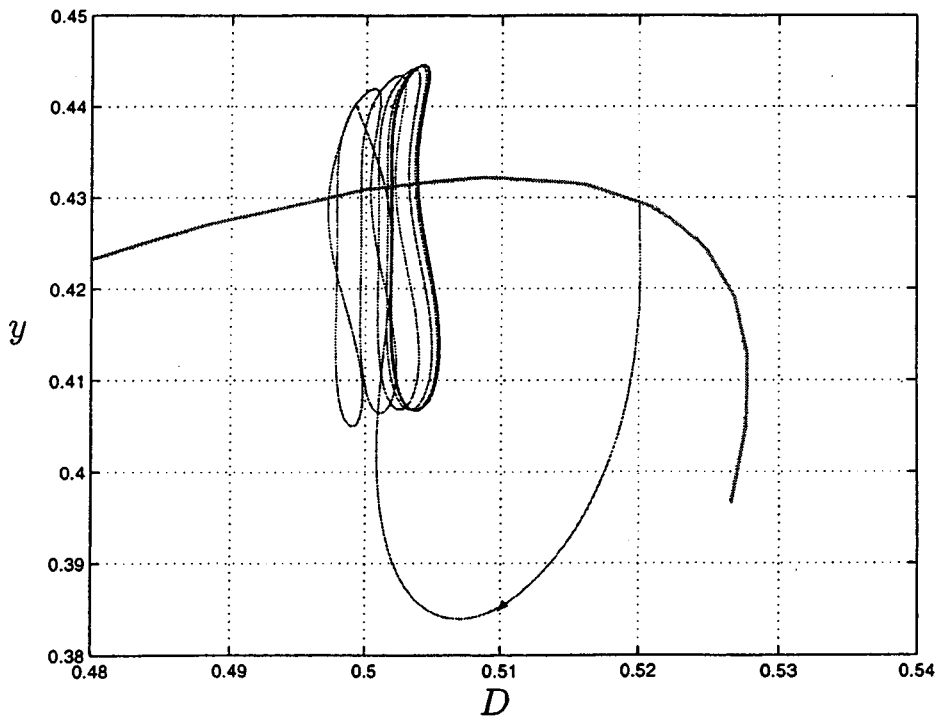

Figure 16. The maximum seeking process in for the Haldane model with state feedback and the initial dilution $D_0 = 0.52$
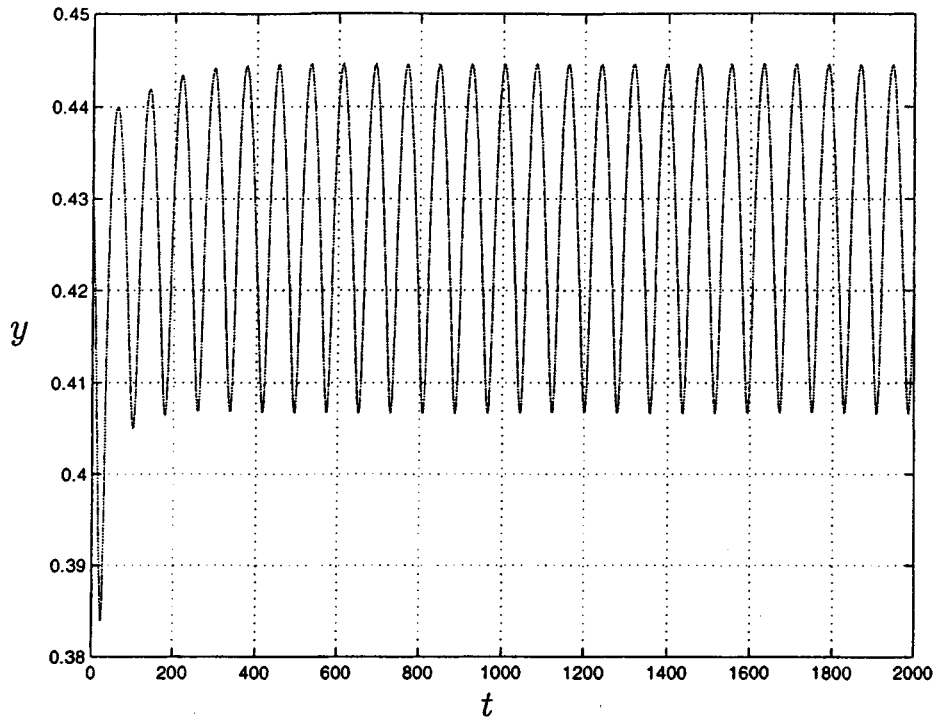
Figure 17. The peak seeking time response of the output with state feedback for the Haldane model with initial dilution rate $D_0 = 0.52$
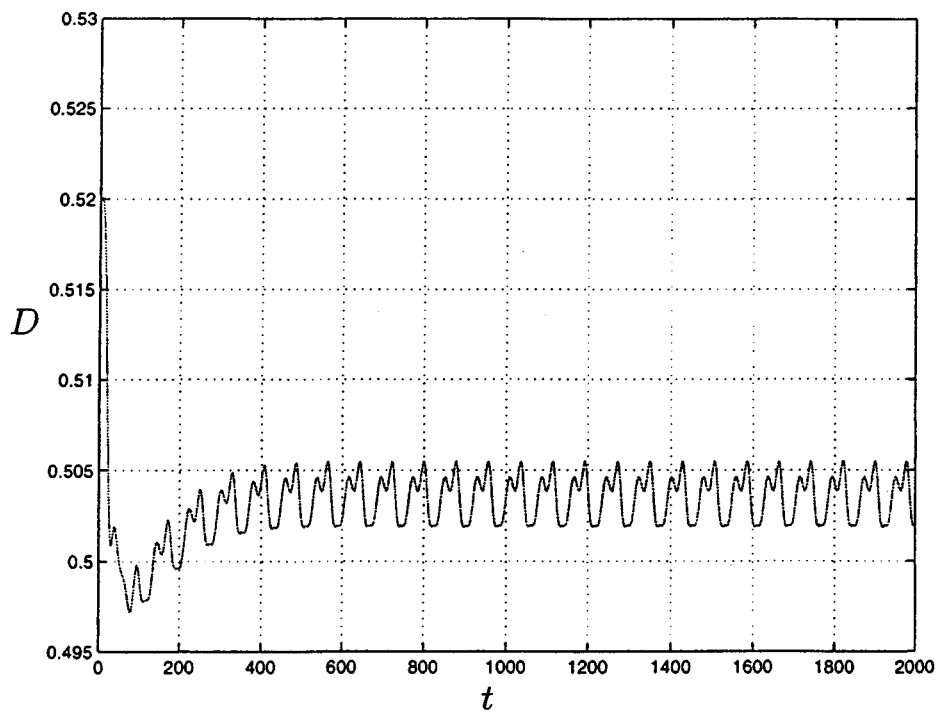

Figure 18. The peak seeking time response of the tuning parameter with state feedback for the Haldane model with initial dilution rate $D_0 = 0.52$

a small amount of stabilizing feedback, drives the system to the optimal equilibrium from a broad region of initial conditions. Thus, the stabilizing feedback improves the operating range of the system.

7. CONCLUSIONS

By applying peak seeking to both Monod and Haldane models, we have shown that it can optimize the steady-state operation of a continuous stirred tank reactor in the face of uncertainty in the kinetics. In the Haldane model, a subcritical bifurcation prevents operation with a satisfactory stability region near the maximum of the biomass outflow rate. For this reason, we apply a local stabilizing feedback to soften the bifurcation. The feedback is passed through a washout filter to keep the same structure of equilibria but only affect their stability type. As a result, the operating range of the system, and the region of applicability of peak seeking, is extended.

As expected from the peak seeking theory, the plots show that $D(t)$ converges to within $O(\omega)$ (on the order of 1%) from D^*.

In all the simulations with peaks seeking, due to the periodic excitation signal, the output undergoes oscillations of less than 5% around the mean value. These oscillations are small relative to the increase in the mean due to peak seeking. Since the oscillations are also relatively small and do not induce excessive wear and tear on the actuator, these oscillations should be of minor concern (unless, of course, the biomass outflow rate is required to be steady, in which case we would turn off the adaptation after the maximum is achieved).

REFERENCES

1. Bastin, G. and J. F. Van Impe, 'Nonlinear and adaptive control in biotechnology: a tutorial', *European J. Control*, 37–53 (1995).
2. Bastin, G. and D. Dochain, *On-line Estimation and Adaptive Control of Bioreactors*, Elsevier Science Publications, Amsterdam, 1990.
3. Chen, L., G. Bastin and V. V. Breusegem, 'A case study of adaptive nonlinear regulation of fed-batch biological reactors', *Automatica*, 55–65 (1995).
4. Van Impe, J. F. and G. Bastin, 'Optimal adaptive control of fed-batch fermentation processes with multiple substrates', *Control Eng. Practice*, 939–954 (1995).
5. Boskovic, J. D. and K. S. Nanendra, 'Comparison of linear, nonlinear and neural-network-based adaptive controllers for a class of fed-batch fermentation processes', *Automatica*, 817–840 (1995).
6. Thibault, J., V. V. Breusegem and A. Chéruy, 'On-line prediction of fermentation variables using neural networks', *Biotechnol. Bioeng.*, 1041–1048 (1990).
7. Yang, Y. Y. and D. A. Linkens, 'Adaptive neural-network-based approach for the control of continuously stirred tank reactor', *IEE Proc. Control Theory Appl.*, **141**, 341–349 (1994).
8. Krstic, M. and H. H. Wang, 'Design and stability analysis of extremum seeking feedback for general nonlinear systems', *Proc. 1997 Conf. on Decision and Control*, San Diego, CA, TA02-3, also *Automatica*, to appear.
9. Wang, H. H., S. Yeung and M. Krstic, 'Experimental application of extremum seeking on an axial-flow compressor', *Proc. 1998 ACC*, Philadelphia, PA, TM09-1.
10. Herbert, D., R. Elsworth and R. C. Telling, 'The continuous culture of bacteria; a theoretical and experimental study', *J. Gen. Microbiol.*, 601–622 (1956).
11. D'Ans, G. and P. Kokotovic, 'Optimal control of bacterial growth', *Automatica*, 729–736 (1972).